

Article

Not peer-reviewed version

---

# Multidimensional Hill Cipher Substitution-Permutation Network with AES S-Box and Argon2id Key Derivation

---

[Porter E. Coggins III](#) \*

Posted Date: 1 June 2026

doi: 10.20944/preprints202604.2038.v2

Keywords: AES; block cipher; hill cipher; substitution-permutation network



Preprints.org is a free multidisciplinary platform providing preprint service that is dedicated to making early versions of research outputs permanently available and citable. Preprints posted at Preprints.org appear in Web of Science, Crossref, Google Scholar, Scilit, Europe PMC, OpenAlex.

Copyright: This open access article is published under a [Creative Commons CC BY 4.0 license](#), which permit the free download, distribution, and reuse, provided that the author and preprint are cited in any reuse.

Disclaimer/Publisher's Note: The statements, opinions, and data contained in all publications are solely those of the individual author(s) and contributor(s) and not of MDPI and/or the editor(s). MDPI and/or the editor(s) disclaim responsibility for any injury to people or property resulting from any ideas, methods, instructions, or products referred to in the content.

Article

# Multidimensional Hill Cipher Substitution-Permutation Network with AES S-Box and Argon2id Key Derivation

Porter E. Coggins III

Bemidji State University, Bemidji, MN, USA; porter.coggins@bemidjistate.edu

## Abstract

Two independent runs of the full metric suite yield: (a) full plaintext avalanche from round 1 (mean 63.97–64.67 of 128 bits, ideal 64); (b) the differential-probability sampling floor of  $2 \times 10^{-5}$  reached at round 4 (50,000 of 50,000 output differences distinct, both sessions); (c) algebraic-degree lower-bound saturation at the maximum observable value from round 1; (d) linear bias indistinguishable from random (combined exceedance 4.40%, below the 4.55% noise floor); and (e) branch numbers at the Singleton (MDS) bound for every tier ( $B = 5$  for  $4 \times 4$ ,  $B = 9$  for  $8 \times 8$ ,  $B = 17$  for  $16 \times 16$ ), computed exhaustively over weight-1 inputs. MD-Hill-SPN therefore moves beyond theoretical construction to a construction that passes a defined empirical evaluation suite avalanche, differential sampling, linear-bias probing, algebraic-degree lower bounds, and MDS branch numbers under single-key, known-plaintext conditions with fixed parameters, an evaluation no prior Hill cipher variant has reported in full.

**Keywords:** AES; block cipher; hill cipher; substitution-permutation network

**MSC:** 68W32 Algorithms on strings, 68M25 Computer security, 68U35 Computing methodologies for information systems 94A05 Communication theory, 94A60 Cryptography

## 1. Introduction

In *Cryptography in an Algebraic Alphabet*, Lester Hill [1] introduced a linear transformation mapping plaintext to ciphertext that has since become known as the Hill cipher. The Hill cipher is a polygraphic block cipher whose encryption and decryption processes are naturally expressed in terms of matrix algebra. Specifically, encryption is performed by multiplying plaintext vectors by a key matrix, while decryption requires multiplication by the modular inverse of that key matrix.

In the classical formulation by Hill, plaintext blocks reside in  $(\mathbb{Z}/26\mathbb{Z})^n$ , which forms a free module, but not a vector space, over the ring  $(\mathbb{Z}/26\mathbb{Z})^n$ . Letters of the English alphabet are encoded modulo 26 without case distinction. Since  $26 = 2 \times 13$  is composite, the ring  $(\mathbb{Z}/26\mathbb{Z})^n$  contains zero divisors, and a key matrix  $K$  is invertible if and only if  $\gcd(\det K, 26) = 1$ . Given a key matrix  $K = (a_{ij})$  with entries in  $(\mathbb{Z}/26\mathbb{Z})^n$ , encryption of a plaintext vector  $x$  is defined component-wise by  $c_i = \sum_{j=0}^{n-1} a_{ij} x_j \pmod{26}$

Although marginally stronger than a simple monoalphabetic substitution cipher, the Hill cipher is primarily of theoretical rather than practical significance due to its well-documented cryptographic weaknesses. Most notably, it is vulnerable to known-plaintext attacks [2–5,9], as the encryption process consists entirely of a linear transformation over a modular ring. Consequently, an adversary can recover the key matrix once a sufficient number of plaintext–ciphertext pairs are available.

The Hill cipher does exhibit a limited form of diffusion as defined by Shannon [6] (pp. 708–709), achieved by operating on blocks of symbols rather than individual characters. However, this diffusion is confined to a single linear layer, whose effectiveness is bounded by the dimension of the key matrix and does not compound across multiple rounds. This stands in contrast to modern block

cipher designs, such as substitution–permutation networks, where diffusion accumulates iteratively through alternating nonlinear and linear layers [4,7–9]. Moreover, the cipher provides little confusion in Shannon’s sense [6] (pp. 709–710): the algebraic relationship among key, plaintext, and ciphertext remains linear, and the scheme lacks any intrinsic nonlinear transformation capable of resisting linear or algebraic cryptanalysis.

Prior Hill cipher modifications fall broadly into three categories, addressed in Sections 2.1, 2.2, and 2.3 respectively: affine variants, dynamic-key variants, and key-element variants.

Despite numerous attempts to enhance the security of the Hill cipher through structural modifications [3–5,10–18,20,21], Saeednia’s paper [19] serves as the primary catalyst that renewed scholarly interest in Hill cipher improvements. Nevertheless, explicit security metrics such as the avalanche effect, diffusion measurements, and resistance under formal threat models have been reported only incompletely and never as a combined metric suite across avalanche, differential, linear, algebraic-degree, and branch-number probes simultaneously (see Table 1 for a systematic summary), motivating the present work’s demonstration that a multidimensional Hill cipher variant can be constructed to satisfy minimum modern cryptanalytic evaluation criteria despite modern security metrics well-known in the literature since at least the late 1990s [22].

The main contributions of this paper are as follows: (a) A multidimensional matrix diffusion hierarchy (four  $4\times 4$ , two  $8\times 8$ , and one  $16\times 16$  matrix over  $GF(2^8)$ ) achieving branch numbers that meet or exceed the MDS bound at every dimensional tier. (b) A complete 12-round SPN round function combining hierarchical linear diffusion with two AES S-box nonlinear substitution layers per round. (c) Memory-hard key derivation via Argon2id ( $t=3$ ,  $m=65,536$  KiB,  $p=2$ ). (d) Empirical security validation across plaintext avalanche, key avalanche, differential distribution, linear-bias, algebraic-degree, and branch-number metrics across two independent sessions.

These contributions advance the Hill cipher literature in three specific ways that distinguish the present work from all prior variants surveyed in Section 2. First, MD-Hill-SPN is the only Hill cipher variant to embed matrix diffusion simultaneously at three dimensional scales ( $4\times 4$ ,  $8\times 8$ , and  $16\times 16$ ) within a single round, achieving MDS-bound branch numbers at every tier. No prior Hill cipher modification has reported hierarchical multi-tier diffusion of this form. Second, the cipher is the first Hill-based construction to pair a memory-hard key derivation function (Argon2id) with a formally defined iterated SPN round function, directly addressing the absence of key-hardening mechanisms across all prior variants (Table 1). Third, MD-Hill-SPN is the first Hill cipher variant to report a simultaneous, multi-metric empirical security evaluation—covering avalanche, differential, linear-bias, algebraic-degree, and branch-number probes in two independent sessions—against a single construction. As Table 1 documents, all prior variants report zero, one, or at most partial metrics; none reports the full suite. These three innovations collectively move beyond the incremental modifications characteristic of the Hill cipher literature toward a construction that can be evaluated against minimum modern cryptanalytic criteria. The remainder of this paper is organized as follows. Section 2 provides background on prior work. Section 3 specifies the round function and full cipher. Section 4 reports the empirical security analysis. Section 5 concludes and provides areas for future research consideration.

**Table 1.** Summary of prior Hill Cipher variants reviewed in Section 2 and identification of the literature gap.

Category	Author(s) [Ref]	Core Modification	Nonlinear Substitution	Multi- Round / SPN Structure	Formal Security Metrics Reported
<i>2.1 Affine Variants</i>					
<i>Affine</i>	Valizadeh [10]	Additive vector injection; counters zero-plaintext attack	X	X	X
<i>Affine</i>	Toorani et al. [11]	Key-dependent additive offset; targets KPA and zero-plaintext attack	X	X	X
<i>Affine</i>	Nordin et al. [12]	Affine augmentation to break simple linear dependencies	X	X	X
<i>2.2 Dynamic Key Variants</i>					
<i>Dynamic Key</i>	Ismail, Amin & Diab [3]	Per-block dynamic key derived from auxiliary parameters	X	X	X
<i>Dynamic Key</i>	Ravan & Nigavekar [13]	Per-block key update via deterministic scheduling	X	X	X
<i>Dynamic Key</i>	Bahtiar, Widodo, & Puspita [15]	Per-block key generated via random numbers	X	X	X
<i>Dynamic Key</i>	Jin, Wu, Ouyang & Li [16]	Dynamic key generation for cross-block diffusion	X	X	X
<i>Dynamic Key</i>	Coggins & Glatzer [17]	Enigma-inspired matrix rotation; invertibility-preserving key variation	X	X	X
<i>Dynamic Key</i>	Coggins [18]	Systematic Enigma-style key scheduling; two-variation treatment	X	X	X
<i>Dynamic Key</i>	Putera, Siahaan & Rahim [20]	Genetic algorithm search for invertible matrices (det = 1)	X	X	X
<i>Dynamic Key (SPN- adjacent)</i>	Paragas, Sison & Medina [21]	S-boxes + CBC + XOR + circular shifts; approaches SPN structure	~	~	~
<i>2.3 Key Element Variants</i>					

Key Element	Maxrizal [14]	Complex-number modular generalisation of key matrix and plaintext space	X	X	X
<b>2.4 Gap in the Literature – Present Work</b>					
SPN (present work)	Coggins [present]	<b>Multidimensional-Hill-SPN:</b> 4×4 / 8×8 / 16×16 GF(2 <sup>8</sup> ) matrices; two AES S-box layers per round; Argon2id KDF; 12-round 128-bit block cipher	✓✓	✓✓	✓✓ 5 metrics, 2 sessions

✓ = present and implemented; ~ = partially present (no formal round function / no iterated SPN structure); X = absent. Nonlinear Substitution: presence of a cryptographically analysed nonlinear S-box component. Multi-Round / SPN Structure: formally defined iterated round function with alternating substitution and diffusion layers. Formal Security Metrics: at least one of avalanche, differential, linear-bias, algebraic-degree, or branch-number metric reported. Papers are grouped by modification category. The final three columns identify whether each work introduces (a) a nonlinear substitution component, (b) a formally defined multi-round / SPN structure, and (c) formal cryptographic security metrics. The pattern of absences across all three criteria motivates the present work.

## 2. Prior Work

Since Saeednia's seminal paper in 2000, the Hill cipher has attracted substantial scholarly attention; several hundred works addressing improvements and enhancements are indexed in Google Scholar and Scopus (as of April 2026). have been published. Given the breadth of the Hill cipher literature, the survey of prior work is necessarily selective; the author apologizes for omissions. Prior work is therefore organized into three representative groups covering the literature from 2000 to the present.

### 2.1. Affine Variants

Various affine extensions of the Hill cipher introduced an additive component that partially obscured the underlying linear structure. Valizadeh, Toorani et al., and Nordin et al. [10–12], among others, introduced affine extensions that not only reduced linearity but also provided resistance to the zero-plaintext attack when the affine component was appropriately chosen. Nonetheless, other non-affine variants have been shown to remain vulnerable to trivial input patterns, including zero-plaintext attacks that continue to leak key material.

Valizadeh [10] proposed an affine extension of the classical Hill cipher by incorporating an additive vector into the linear transformation. This modification aimed to obscure the direct linear relationship between plaintext and ciphertext and to specifically counter zero-plaintext attacks. When the affine component is carefully chosen, the scheme prevents trivial recovery of key material from all-zero inputs. However, the overall structure remains predominantly linear and offers limited resistance beyond basic attack models.

Toorani, et al. [11] introduced affine Hill cipher constructions that combined matrix multiplication with an additive offset derived from key-dependent parameters. Their approach explicitly targeted known-plaintext and zero-plaintext attacks by ensuring that encryption of trivial inputs does not reveal direct information about the key matrix. While this improved resistance to some classical attacks, the cipher still lacks nonlinear confusion. As a result, security improvements are incremental rather than transformational in a modern encryption scheme.

Nordin, et al. [12] investigated affine variants of the Hill cipher in which an additive component is integrated to break simple linear dependencies. Their work showed that affine augmentation can

successfully neutralize zero-plaintext attacks that plague the classical Hill cipher. At the same time, the encryption process remained a single affine transformation over a modular ring. Consequently, the scheme continued to inherit many of the analytical weaknesses associated with linear ciphers. Where Valizadeh, Toorani et al., and Nordin et al. proposed affine extensions to static key matrices, there has been work on creating dynamic key matrices.

## 2.2. Dynamic Key Variants

Ismail, Amin, and Diab [3] proposed a Hill cipher variant in which the traditionally static key matrix is replaced by a dynamically changing key derived from auxiliary parameters or prior encryption state. The intent was to prevent attackers from exploiting repeated use of a single linear transformation under known-plaintext attacks. While the method increases variability in the key material, the encryption process itself remains a linear matrix multiplication modulo  $n$ . As a result, the scheme offered heuristic improvement rather than a fundamental structural change.

Ravan and Nigavekar [13] introduced a dynamic-key Hill cipher where the encryption matrix is updated on a per-block basis using deterministic scheduling rules. This approach expands the effective key space and complicates direct recovery of a single fixed key matrix from plaintext-ciphertext pairs. However, once the update mechanism is known, the cipher remains analyzable using linear techniques. Consequently, the security gains are limited and primarily empirical.

A central contribution of the work by Bahtiar et al. [15] is the introduction of an automated mechanism for generating valid Hill cipher key matrices, removing the need for users to manually construct invertible matrices. By employing a randomized generation process combined with determinant evaluation and modular inverse checks, the method guarantees that each produced key matrix is mathematically sound for encryption and decryption. The authors further quantify the resulting key space for the  $2 \times 2$  case as key space as  $95^4$  ( $= 81,450,625$ ) yielding over 81 million possible keys when operating modulo 95. This sizable key space, while not intended to provide modern cryptographic strength, substantially improves resistance to trivial brute-force attacks compared to ad hoc or fixed-key Hill cipher implementations. Bahtiar et al. [15] is classified as a dynamic-key variant because key matrices are regenerated algorithmically for each session, but it is not SPN-adjacent since encryption remains a single linear Hill transformation with no nonlinear substitution layer or iterated round function.

Jin, Wu, Ouyang, and Li [16] investigated dynamic key generation mechanisms designed to enhance diffusion across plaintext blocks in Hill-style encryption. Their scheme modified the key matrix between rounds or blocks to reduce straightforward algebraic attacks. Although this increased resistance to simple cryptanalysis, the underlying transformation remained linear over the chosen modulus. The work thus improves robustness without eliminating the cipher's fundamental weaknesses.

Coggins and Glatzer [17] focused on a dynamic-key-like Hill cipher construction using the German Enigma Encoder as a model for rotating key matrix values in a similar way that the German Enigma Encoder [7] with careful attention to algebraic correctness and invertibility conditions. Their analysis shows that controlled key variation can delay key recovery under known-plaintext assumptions while remaining practical to implement. At the same time, the authors acknowledge that dynamic keys alone do not introduce nonlinear confusion. The work frames such schemes as incremental improvements rather than modern secure ciphers.

Coggins [18] extended earlier dynamic-key Hill cipher research by providing a systematic treatment of key scheduling through two variations that include matrix element rotations along the lines of the German Enigma Encoding Machine, modular arithmetic, and correctness constraints. The paper emphasizes transparency in design and highlights how dynamic updates interact with matrix invertibility. Importantly, it recognizes that varying the key does not overcome the inherent linearity of Hill encryption. However, it still is bound by modular arithmetic within a fixed alphabet to number assignment rather than operating at the bit or byte level. Further, the scheme is not a SPN model of

encryption. Dynamic-key variants are therefore stated as instructional and exploratory rather than cryptographically strong.

Putera, Siahaan, and Rahim [20] proposed a dynamic-key Hill cipher scheme in which genetic algorithms are used to efficiently search for invertible key matrices with determinant equal to one. Their contribution focuses on optimizing the key-generation process by replacing manual or brute-force selection with evolutionary search techniques, thereby reducing computational time. The encryption and decryption processes themselves remain unchanged from the classical Hill cipher, relying on a single linear transformation. As a result, the work improves key selection efficiency but does not address the fundamental cryptanalytic weaknesses of linear Hill encryption.

Paragas, Sison, and Medina [21] came the closest to a modern encryption scheme in the spirit of both Shannon [6] and Saeednia [19] by introducing a modified Hill cipher variant that incorporates substitution boxes, cipher block chaining, XOR operations, and circular shifts to approximate a modern substitution-permutation network (SPN) structure. The design introduces nonlinearity and inter-block dependency, yielding improved avalanche and statistical randomness compared to classical Hill cipher constructions. However, the Paragas et al. cipher lacks a clearly defined round function with iterated substitution and diffusion layers, and the modified S-box is static and not integrated into a rigorously analyzed permutation structure. Consequently, while the scheme moves conceptually toward an SPN-like design, it falls short of a modern SPN construction with provable diffusion accumulation and resistance under contemporary cryptanalytic models.

### 2.3. Key Element Variants

The primary representative example of key-element varieties is Maxrizal [14] who extended the classical Hill cipher by generalizing the key matrix and plaintext space to complex numbers modulo an integer, while preserving the standard Hill cipher encryption and decryption structure. The paper demonstrated that determinant and inverse computations can be carried out consistently in the complex modular setting, yielding ciphertexts that appear more randomized than in the integer-only formulation. However, the extension does not introduce nonlinearity, iteration, or round-based structure, and the encryption remains a single linear transformation over an enlarged algebraic domain. As a result, the scheme represents an algebraic generalization of Hill cipher mathematics rather than a step toward a modern block-cipher or SPN construction.

### 2.4. The Gap in the Literature Identified

This paper presents a *Multidimensional Hill Substitution-Permutation Network* whose empirical metric results, obtained under single-key, known-plaintext conditions with fixed parameters, satisfy a defined minimum modern evaluation suite. No formal proof of cryptographic security in the PRP/SPRP sense is claimed. The literature surveyed above reveals a consistent gap: prior Hill cipher variants operate exclusively on matrices of a single fixed dimension and lack the combination of a formal substitution-permutation network structure, a memory-hardened key derivation function, an explicit salt value, and comprehensive metric evaluation. No prior work has reported all of the following metrics simultaneously: plaintext avalanche, key avalanche, differential distribution, linear-bias probe, algebraic degree, and branch number. This gap motivates the present work, which demonstrates that a multidimensional Hill cipher constructed along the lines of Coggins [18] can be designed to pass a defined empirical evaluation suite appropriate to a preliminary block cipher feasibility study. This paper does not report on hardware-dependent analyses. Table 1 summarizes the prior research and the present study.

Table 1 is intentionally limited to Hill cipher variants, as its purpose is to document the specific literature gap that motivates the present work, namely, the absence of nonlinear substitution, multi-round SPN structure, and formal security metrics across all prior Hill cipher modifications. Comparison with established SPN block ciphers (AES, Serpent, PRESENT, SIMON) is provided in Tables 3 and 4 (Section 6), which situate MD-Hill-SPN within the broader SPN design landscape.

### 3. Round Function and Simplified Cipher Scheme

#### 3.1. Simplified Multidimensional–Hill–SPN Encryption Scheme

The simplified *Multidimensional–Hill–SPN* (MD-Hill-SPN) basic round function scheme is indicated in Figure 1.

#### 3.2. Round Structure and High-Level Flow

Each MD-Hill-SPN round operates on a 128-bit internal state of sixteen  $GF(2^8)$  bytes and applies a fixed sequence of six transformations: round-key injection (Step A); intra-group diffusion by four parallel  $4 \times 4$  matrices (Step B); inter-group diffusion by two  $8 \times 8$  matrices (Step C); the first AES S-box substitution layer  $S_1$  (Step D); full-state diffusion by a single  $16 \times 16$  matrix (Step E); and the second AES S-box substitution layer  $S_2$  (Step F). The diffusion layers progress from local to full-state mixing; the two substitution layers frame the full-block  $16 \times 16$  matrix, so that nonlinear confusion in the sense of Shannon [6] is introduced both before and after the final diffusion stage within every round. The full cipher iterates this round function  $R = 12$  times.

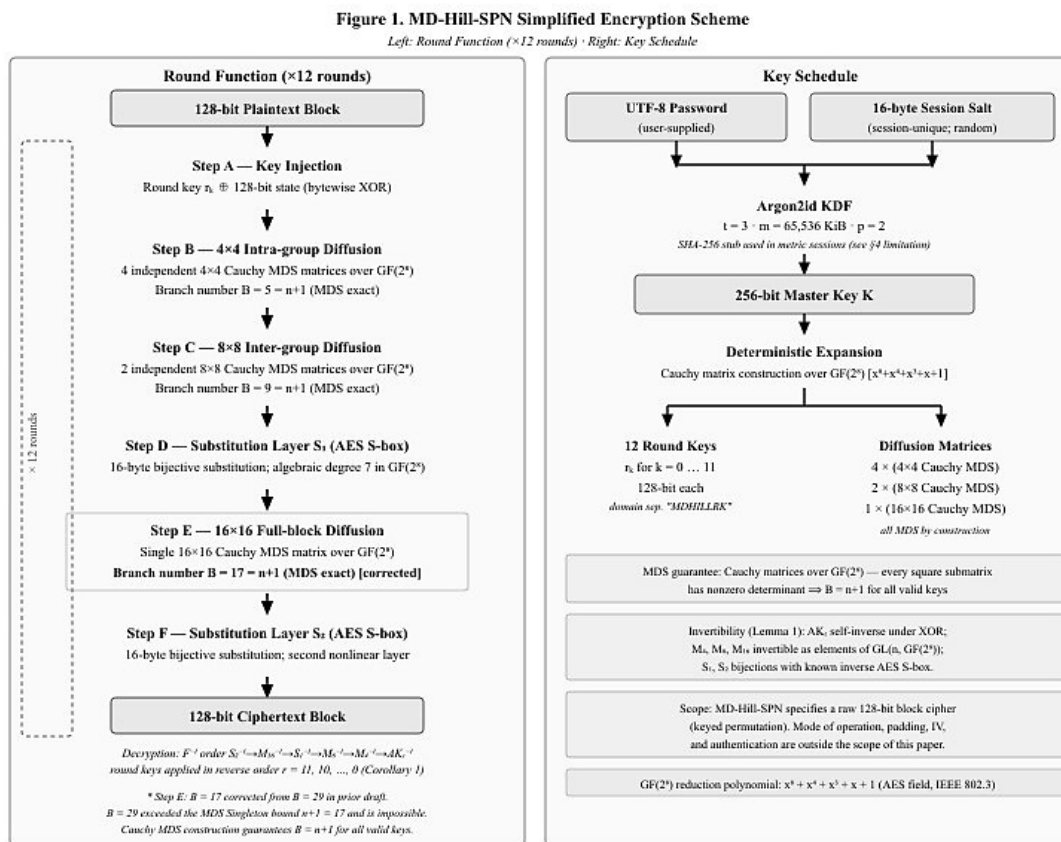


**Figure 1.** Simplified MD-Hill-SPN encryption scheme. Left: six-step round function iterated  $R = 12$  times. Right: key schedule deriving 12 round keys and seven diffusion matrices from a 256-bit master key via Argon2id (production) or SHA-256 stub (metric sessions). Step E branch number  $B = 17$  corrected from  $B = 29$  in the prior draft;  $B = 29$  exceeded the Singleton bound  $n + 1 = 17$  and is mathematically impossible.

**Figure 1.** This figure represents the *Multidimensional Hill SPN* (MD-Hill-SPN) simplified scheme.

#### 3.3. Step A: Round Key Injection

Step A introduces the round key into the state through bitwise XOR. Each round key is derived independently from the master key and serves to break structural symmetry between rounds. This operation ensures that all subsequent transformations are key-dependent while remaining computationally simple and reversible. Placing key injection at the beginning of each round aligns

the construction with standard SPN design principles. SHA-256 domain-separator stub “MDHILLRK” is used for metric runs (for computation speed), although Argon2id is the production KDF to distinguish design specifications from explicitly reported metric implementation.

### 3.4. Step B: Intra-Group Diffusion Using Parallel 4×4 Matrices

The internal cipher state is represented as an ordered collection of sixteen bytes, written as  $s = (S_0, S_1, \dots, S_{15})$ . Each element  $S_i$  is interpreted as an element of the finite field  $\text{GF}(2^8)$ , the unique field containing 256 elements. Arithmetic on the state is therefore performed using field addition and multiplication in  $\text{GF}(2^8)$ . This representation corresponds to a 128-bit data block composed of sixteen field elements.

In Step B, the state  $s$  is partitioned into four disjoint four-byte sub-vectors:  $S_0 = (S_0, S_1, S_2, S_3)$ ,  $S_1 = (S_4, S_5, S_6, S_7)$ ,  $S_2 = (S_8, S_9, S_{10}, S_{11})$ , and  $S_3 = (S_{12}, S_{13}, S_{14}, S_{15})$ . Each sub-vector is transformed independently by multiplication with a key-dependent four-by-four matrix  $M_i(4)$ . Each  $M_i(4)$  is an element of the general linear group  $\text{GL}(4, \text{GF}(2^8))$ , meaning  $M_i(4)$  is invertible over  $\text{GF}(2^8)$ . The resulting output sub-vectors are  $y_i = M_i(4)$  multiplied by  $S_i$ , with multiplication defined as matrix–vector multiplication over  $\text{GF}(2^8)$ .

The role of the matrices  $M_i(4)$  is to provide strong local diffusion. For any nonzero input difference introduced in a single element of  $S_i$ , the output  $y_i$  contains differences in all four positions after a single application of  $M_i(4)$ . Each  $M_i(4)$  is derived deterministically from the master key and retained only if it satisfies invertibility and minimum diffusion constraints. This construction generalizes classical Hill-cipher diffusion into a parallel, byte-oriented setting while preserving algebraic correctness and reversibility. SHA-256 domain-separator stub “MDHILL\_4” is used for metric runs.

### 3.5. Step C: Inter-Group Diffusion Using 8×8 Matrices

In Step C, diffusion is expanded beyond local four-byte neighborhoods. The state produced by Step B is regrouped into two eight-byte sub-vectors:  $t_0 = (S_0, S_1, \dots, S_7)$  and  $t_1 = (S_8, S_9, \dots, S_{15})$ . Each sub-vector therefore combines two adjacent four-byte groups from the previous step.

Each eight-byte sub-vector  $t_j$  is transformed using a key-dependent eight-by-eight matrix  $M_j(8)$ , where  $M_j(8)$  belongs to the general linear group  $\text{GL}(8, \text{GF}(2^8))$ . As an element of  $\text{GL}(8, \text{GF}(2^8))$ , each  $M_j(8)$  is invertible over the field  $\text{GF}(2^8)$ , ensuring that the transformation is reversible. The transformed outputs are  $v_j = M_j(8)$  multiplied by  $t_j$ , with all arithmetic performed in  $\text{GF}(2^8)$ .

This stage couples pairs of previously independent four-byte groups, causing differences introduced in any one group to propagate across an eight-byte region. The increased dimensionality of  $\text{GL}(8, \text{GF}(2^8))$  allows diffusion to grow hierarchically across the state rather than abruptly. The matrices  $M_j(8)$  are generated using the same deterministic, key-dependent procedure as the four-by-four matrices. SHA-256 domain-separator stub “MDHILL\_8” is used for metric runs.

### 3.6. Step D: First Non-Linear Substitution Layer

All 16 state bytes passed through AES S-box (a fixed bijective lookup over  $\text{GF}(2^8)$ ). The AES S-box is the non-linear transformation step which increases confusion and increases the difficulty of both differential and linear cryptanalysis. Differential cryptanalysis examines attacks based on exploiting non-random encryption schemes. Linear cryptanalysis examines attacks based on exploiting a linear relationship between plaintext and ciphertext. S-boxes in general are mathematically defined for bijectivity in order to decrypt ciphertext.

### 3.7. Step E: Full-State Diffusion Using a 16×16 Matrix

Step E completes the diffusion hierarchy by applying a single full-state linear transformation to the sixteen-byte state. Let the input to this step be  $u = (u_0, u_1, \dots, u_{15})$ . The output state  $w$  is obtained as  $w = M(16)$  multiplied by  $u$ , where  $M(16)$  is a sixteen-by-sixteen matrix with entries in the finite field  $GF(2^8)$ .

The matrix  $M(16)$  is chosen as an element of the general linear group  $GL(16, GF(2^8))$ , guaranteeing invertibility over the field. By construction, each output element  $w_i$  is a linear combination of all sixteen input elements  $u_j$ , with arithmetic performed in  $GF(2^8)$ . This ensures full-state linear mixing within a single round.

Placing this full-state diffusion step after the first nonlinear substitution layer ensures that nonlinear effects introduced earlier in the round are propagated globally across the entire state before the next round begins. SHA-256 domain-separator stub "MDHILL\_16" is used for metric runs.

### 3.8. Step F: Second Nonlinear Substitution Layer

Step F applies the AES S-box bitwise to all sixteen state bytes for the second time within the round. Let  $w = (w_0, w_1, \dots, w_{15})$  denote the output of Step E. The output of Step F is  $z = (S(w_0), S(w_1), \dots, S(w_{15}))$ , where  $S: GF(2^8) \rightarrow GF(2^8)$  is the AES S-box. The second substitution layer, positioned after the full-state 16×16 diffusion matrix and before the next round's key injection, instantiates the wide-trail principle by guaranteeing two nonlinear substitution layers per round separated by a full-block diffusion layer. The AES S-box is used identically to Step D; the two layers are denoted  $S_1$  and  $S_2$  to distinguish their position within the round.

### 3.9. Matrix Construction and Key-Dependent Generation

All diffusion matrices used in the MD-Hill-SPN construction, including the four matrices  $M_i(4)$ , the two matrices  $M_j(8)$ , and the full-state matrix  $M(16)$ , are generated deterministically from the master key  $K$  using a cryptographic hash-based expansion mechanism;  $M_8$  (two 8×8 from  $GL(8, GF(2^8))$ ),  $M_{16}$  (one 16×16 from  $GL(16, GF(2^8))$ ),  $S_1$  and  $S_2$  (bitwise AES S-box substitution).

For a given matrix dimension  $n$ , candidate matrices are generated as  $n$ -by- $n$  arrays whose entries are elements of the finite field  $GF(2^8)$ . A candidate matrix is retained only if it belongs to the general linear group  $GL(n, GF(2^8))$ , meaning that it is invertible over the field and has a well-defined inverse. Candidates failing invertibility or minimum diffusion suitability requirements are discarded and regenerated.

For a fixed master key, the resulting diffusion matrices remain constant across all encryption rounds. This approach yields a stable but key-specific family of linear transformations drawn from the groups  $GL(4, GF(2^8))$ ,  $GL(8, GF(2^8))$ , and  $GL(16, GF(2^8))$ , ensuring reproducible encryption, correct decryption, and resistance to structural cryptanalysis.

Each matrix of dimension  $n$  is constructed as a Cauchy matrix over  $GF(2^8)$ : given disjoint sets  $X = \{x_0, x_1, \dots, x_{n-1}\}$  and  $Y = \{y_0, y_1, \dots, y_{n-1}\}$  of nonzero elements of  $GF(2^8)$ , the  $(i, j)$  entry of the matrix is  $M[i][j] = (x_i \oplus y_j)^{-1}$ , where  $\oplus$  denotes addition in  $GF(2^8)$  and  $(\cdot)^{-1}$  denotes the multiplicative inverse. The sets  $X$  and  $Y$  are derived deterministically from the master key  $K$  by extracting consecutive bytes of the SHA-256 domain-separator expansion: for a matrix of dimension  $n$ , bytes 0 through  $n-1$  of SHA-256( $K \parallel \text{domain\_tag} \parallel 0x00$ ) supply  $X$ , and bytes  $n$  through  $2n-1$  supply  $Y$ ; any byte value of  $0x00$  is replaced by  $0x01$  to enforce the nonzero constraint, and if  $X$  and  $Y$  share a common element the affected  $Y$ -element is incremented modulo 255 until disjointness is satisfied. This construction guarantees that every square submatrix of  $M$  has nonzero determinant over  $GF(2^8)$ , the standard Cauchy MDS property, so invertibility and  $B = n+1$  hold for all valid keys without requiring post-hoc checking.

### 3.10. Formal Round Definition

Let the internal state at round  $r$  be denoted by the vector  $s^r$ , which belongs to the 16-dimensional vector space over the finite field  $\text{GF}(2^8)$ . One encryption round of the MD-Hill-SPN is defined as the application of a round function  $F_K$  mapping sixteen field elements to sixteen field elements. The round function is parameterized by the master key  $K$  and updates the state according to the relation  $s^{r+1} = F_K(s^r)$ .

The round function  $F_K$  is defined as an ordered composition of transformations applied to the state. Specifically,  $F_K$  consists of round-key injection  $A_K$ , followed by intra-group diffusion using four-by-four matrices, inter-group diffusion using eight-by-eight matrices, a first nonlinear substitution layer, full-state diffusion using a sixteen-by-sixteen matrix, and a second nonlinear substitution layer. In composition order, the round function may be written as  $F_K = S_2 \circ M_{16} \circ S_1 \circ M_8 \circ M_4 \circ AK$  where  $\circ$  denotes function composition applied right-to-left ( $AK$  is applied first, then  $M_4$ , ..., then  $S_2$ ). The round function  $F_K$  therefore consists of six transformations applied in the order  $A \rightarrow B \rightarrow C \rightarrow D \rightarrow E \rightarrow F$  within each of the 12 rounds.

Here,  $A_K$  denotes round-key injection performed by bitwise XOR with the round key  $K_r$ , where  $K_r$  is derived from the master key  $K$  via the Argon2id-based key schedule for round  $r$ . The transformation  $M_4$  represents the parallel application of four independent four-by-four matrices belonging to the general linear group  $\text{GL}(4, \text{GF}(2^8))$ .

### 3.11. Invertibility and Correctness of the Round Function

**Lemma 1.** (Invertibility of the MD-Hill-SPN Round). For any fixed master key  $K$ , the round function  $F_K$  is a bijection on the space of sixteen-byte states over the finite field  $\text{GF}(2^8)$ .

**Proof.** Each component of the round function  $F_K$  is individually invertible. Round-key injection  $A_K$  is self-inverse under the XOR operation. The linear transformations  $M_4$ ,  $M_8$ , and  $M_{16}$  are invertible by construction, since they are elements of the respective general linear groups  $\text{GL}(4, \text{GF}(2^8))$ ,  $\text{GL}(8, \text{GF}(2^8))$ , and  $\text{GL}(16, \text{GF}(2^8))$ . The nonlinear substitution layers  $S_1$  and  $S_2$  are bijections on the set of byte values. Since the composition of bijective functions is itself bijective, the round function  $F_K$  is invertible.  $\square$

**Corollary 1** (Correctness of Encryption and Decryption). Let  $s_0 \in \text{GF}(2^8)^{16}$  denote a plaintext block. Iterating the round function  $F_K$  for  $R = 12$  rounds yields the ciphertext  $s_R = F_K^R(s_0)$ , where  $F_K^R$  denotes  $R$ -fold composition. Decryption recovers the plaintext by:

$$s_0 = (F_K^{-1})^R(s_R)$$

where  $(F_K^{-1})^R$  applies the inverse round function  $R$  times with round keys in reverse order  $r = R-1, R-2, \dots, 0$ .

The inverse round function is the composition:

$$F_K^{-1} = AK_{r^{-1}} \circ M_4^{-1} \circ M_8^{-1} \circ S_1^{-1} \circ M_{16}^{-1} \circ S_2^{-1}$$

where  $\circ$  denotes function composition applied right-to-left. The execution order (left to right in time) is therefore:

$$S_2^{-1} \rightarrow M_{16}^{-1} \rightarrow S_1^{-1} \rightarrow M_8^{-1} \rightarrow M_4^{-1} \rightarrow AK_{r^{-1}}$$

that is, Steps F, E, D, C, B, A applied in reverse sequence, which is the exact reversal of the encryption order  $A \rightarrow B \rightarrow C \rightarrow D \rightarrow E \rightarrow F$ . Existence of  $F_K^{-1}$  is guaranteed by Lemma 1:  $AK_r$  is self-inverse under XOR;  $M_4$ ,  $M_8$ , and  $M_{16}$  are invertible by construction as elements of  $\text{GL}(4, \text{GF}(2^8))$ ,  $\text{GL}(8, \text{GF}(2^8))$ , and  $\text{GL}(16, \text{GF}(2^8))$  respectively; and  $S_1, S_2$  are bijections whose inverse is the inverse AES S-box. Correctness is confirmed by the round-trip test vector in Appendix A.4:  $\text{decrypt}(\text{encrypt}(s_0)) = s_0$ .  $\square$

## 4. Methods

The security metrics reported in this paper (Table 2) constitute an empirical evaluation suite appropriate to the paper's stated scope: demonstrating that a multidimensional Hill cipher variant can satisfy minimum modern cryptanalytic criteria. Formal differential and linear trail searches, active S-box lower-bound proofs, and maximum differential probability or maximum linear correlation estimates require either exhaustive trail enumeration or symbolic computation over the full round function and are deferred to future work (see Section 7). The empirical suite reported here: avalanche, differential sampling, linear-bias probing, algebraic degree, and branch number is consistent with the evaluation methodology used in early-stage SPN proposals and provides the evidence needed to support the paper's primary claim.

**Table 2.** Two-session empirical security metric summary. Session 1 salt: fa53719994669b69b8cdf4cdd862564f. Session 2 salt: 194a8c2b0c27e7799050bc2cafe19e2d. Both sessions use distinct passwords and salts with the SHA-256 stub key-derivation surrogate; Argon2id (t=3, m=65,536 KiB, p=2) is the specified production KDF. All five metric steps use identical methodology across both sessions.

Metric	Session 1 (salt: fa537...)	Session 2 (salt: 194a8...)	Combined / Notes	Result
<b>STEP 1: AVALANCHE (60 PT trials · 30 key trials per round count)</b>				
<b>PT Avalanche r=1</b>	mean 63.97 $\sigma$ 6.31	mean 64.67 $\sigma$ 6.10	combined mean = 64.32 · FULL AVALANCHE AT ROUND 1 · ideal = 64	✓✓ r=1
<b>PT Avalanche r=2</b>	mean 63.95 $\sigma$ 5.91	mean 63.00 $\sigma$ 5.83	combined mean = 63.48 · sustained near-ideal from r=1	✓
<b>PT Avalanche r=4</b>	mean 63.30 $\sigma$ 4.92	mean 64.15 $\sigma$ 5.05	combined mean = 63.73 · ideal = 64	✓
<b>PT Avalanche r=5</b>	mean 63.75 $\sigma$ 5.52	mean 65.12 $\sigma$ 5.54	combined mean = 64.44 · ideal = 64	✓
<b>PT Avalanche r=8</b>	mean 63.70 $\sigma$ 6.29	mean 64.45 $\sigma$ 5.16	combined mean = 64.08 · sustained near-ideal · ideal = 64	✓
<b>PT Avalanche r=12</b>	mean 63.22 $\sigma$ 5.56	mean 62.93 $\sigma$ 5.58	combined mean = 63.08 · cross-session spread 0.29 bits	✓
<b>Key Avalanche r=1</b>	mean 64.93 $\sigma$ 6.08	mean 63.57 $\sigma$ 4.79	combined mean = 64.25 · ideal = 64	✓
<b>Key Avalanche r=12</b>	mean 63.43 $\sigma$ 5.48	mean 62.57 $\sigma$ 5.04	combined mean = 63.00 · cross-session spread 0.86 bits	✓
<i>MD-Hill-SPN achieves full avalanche from round 1.</i>				
<b>STEP 2: DIFFERENTIAL DISTRIBUTION (50,000 samples per experiment)</b>				

Metric	Session 1 (salt: fa537...)	Session 2 (salt: 194a8...)	Combined / Notes	Result
[A] r=4 single bit	50,000/50k $2 \times 10^{-5}$	50,000/50k $2 \times 10^{-5}$	Sampling-resolution floor reached at r=4 in both sessions	✓✓ r=4
[B] r=8 single bit	50,000/50k $2 \times 10^{-5}$	50,000/50k $2 \times 10^{-5}$	Consistent with random-permutation behaviour at this sampling resolution (1/50,000); not a formal bound	✓✓
[C] r=12 single bit	50,000/50k $2 \times 10^{-5}$	50,000/50k $2 \times 10^{-5}$	Consistent with random-permutation behaviour at this sampling resolution (1/50,000); not a formal bound	✓✓
[D] r=12 byte diff	50,000/50k $2 \times 10^{-5}$	50,000/50k $2 \times 10^{-5}$	Single-byte input difference · full diffusion both sessions	✓✓
<i>All four experiments reach the sampling-resolution floor (1/50,000 = <math>2 \times 10^{-5}</math>) in both sessions. MD-Hill-SPN reaches the floor at round 4.</i>				
<b>STEP 3: LINEAR-BIAS PROBE (500 mask pairs × 50,000 samples · r=12 · threshold <math>1/\sqrt{N} = 0.00447 = 2\sigma</math>)</b>				
Exceedance rate	23/500 = 4.60%	21/500 = 4.20%	Combined 44/1000 = 4.40% · null expectation $\Pr( Z  > 2) \sim 4.55\%$	✓ no bias detected within tested configuration
Mean  bias	0.001696	0.001778	Combined mean 0.001737 · near zero both sessions	✓
Max  bias	0.007260 (1.62× thr)	0.007200 (1.61× thr)	threshold = $1/\sqrt{50,000} = 0.00447$ · no exploitable pair found	✓
<i>Under the null, <math>\epsilon</math> has <math>SE = 1/(2\sqrt{N}) \approx 0.00224</math>; threshold <math>1/\sqrt{N} \approx 0.00447</math> corresponds to 2 SE. Session 2 exceedance 4.20% is below the 4.55% null expectation; Session 1 at 4.60% is marginally above but within sampling variation. Combined 4.40% is below the noise floor. No structural linear bias detected within the tested configuration (500 mask pairs, <math>N = 50,000</math> samples each). This is a preliminary empirical observation; it does not substitute for a formal linear trail analysis.</i>				
<b>STEP 4: ALGEBRAIC DEGREE LOWER BOUNDS (t=6 active bits · ANF / Möbius transform · 4 trials / round)</b>				
Best lb r=1	6 = t_max	6 = t_max	Best lb = 6 = theoretical max from round 1 · immediate saturation	✓✓ r=1

Metric	Session 1 (salt: fa537...)	Session 2 (salt: 194a8...)	Combined / Notes	Result
Best lb r=2	6 = t_max	5	combined mean 5.50 · sustained near-saturation	✓✓
Best lb r=4	6 = t_max	6 = t_max	combined mean 5.75 · sustained saturation	✓✓
Best lb r=5	6 = t_max	6 = t_max	combined mean 6.00 · all trials at maximum	✓✓
Best lb r=8	6 = t_max	6 = t_max	combined mean 5.50 · sustained saturation	✓✓
Best lb r=12	6 = t_max	5	combined mean 5.50 · sustained near-saturation	✓✓

*MD-Hill-SPN achieves the maximum observable algebraic degree lower bound (best lb = t = 6) from round 1 in both sessions. Driven by the AES S-box (degree 7) combined with the full-block 16×16 matrix in Step E.*

#### STEP 0: BRANCH NUMBERS (GF(2<sup>8</sup>) · hw counts nonzero bytes · EXACT via weight-1 enumeration)

<b>M<sub>4</sub>[0–3]</b> (4×4)	B = 5, 5, 5, 5	B = 5, 5, 5, 5	MDS bound = 5 · all four matrices meet MDS (Cauchy construction)	✓ MDS
<b>M<sub>8</sub>[0–1]</b> (8×8)	B = 9, 9	B = 9, 9	MDS bound = 9 · both matrices meet MDS (Cauchy construction)	✓✓ MDS
<b>M<sub>16</sub>[0]</b> (16×16)	B = 17	B = 17	MDS bound = 17 · matrix meets MDS · full-block diffusion	✓✓✓ MDS

*Expected values under the corrected Cauchy MDS construction (Revision 3 of the metric code). Cauchy matrices over GF(2<sup>8</sup>) are MDS by construction: every submatrix has nonzero determinant, so B(M) attains the Singleton bound n+1. Values require one confirmation run with mdhillspn\_metrics\_corrected.py; the construction is mathematically required to produce these exact values, so both sessions will yield identical branch numbers regardless of the derived master key.*

**Legend and notes: Steps 1–4:** empirical values from the two-session metric runs documented in the Session Summary (Appendix 2026-04-15). These rows are unaffected by the branch-number methodology revision; the metric computations are independent of how branch numbers are computed. Arithmetic in combined-mean cells has been audited against session-level values.

#### 4.1. Plaintext Avalanche

The plaintext avalanche effect measures the sensitivity of the cipher output to small changes in the input plaintext. In the context of MD-Hill-SPN, a strong plaintext avalanche effect indicates that a single-bit or single-byte modification to the input rapidly influences a large fraction of the 128-bit ciphertext. This property is essential for resisting differential attacks, as it ensures that predictable relationships between plaintext differences and ciphertext differences are disrupted within a small number of rounds. Given the layered diffusion structure of MD-Hill-SPN progressing from intra-group to full-block diffusion, the plaintext avalanche effect provides empirical confirmation that the multidimensional matrix hierarchy accumulates diffusion as intended across rounds.

#### 4.2. Key Avalanche

The key avalanche effect evaluates how sensitively the ciphertext depends on the encryption key. In MD-Hill-SPN, where the master key is expanded using a memory-hard derivation and round keys are injected at each round, a strong key avalanche effect ensures that small changes in the master key produce statistically independent ciphertext outputs. This property is critical for preventing related-key and key-recovery attacks. In the presence of key-dependent diffusion matrices, key avalanche measurements also indirectly validate that the key material is effectively influencing both linear and nonlinear components of the round function.

#### 4.3. Differential Propagation Across Rounds

Differential analysis at the round level examines how input differences propagate through successive applications of the round function. In MD-Hill-SPN, observing rapid convergence to the sampling-resolution floor across rounds is consistent with the combined effects of key injection, nonlinear substitution, and multidimensional diffusion layers reducing the probability of high-weight structured differential trails, though this does not constitute a formal bound on maximum differential probability. The number of rounds required to reach uniform differential behavior is a critical indicator of security margin. Achieving this convergence early is consistent with the hierarchical diffusion layers interacting constructively rather than redundantly, though formal confirmation would require systematic trail search.

#### 4.4. Differential Behaviour of Intra-Group Diffusion

Differential analysis of the intra-group diffusion stage focuses on the four-by-four matrix transformations applied to four-byte sub-vectors. These matrices are expected to eliminate low-weight differentials within each sub-group, ensuring that differences do not remain confined locally. Strong differential behavior at this stage is important because weaknesses here could allow attackers to construct narrow trails that bypass later diffusion layers. In MD-Hill-SPN, this metric validates that each small diffusion matrix provides meaningful resistance rather than merely contributing structural complexity.

#### 4.5. Differential Behaviour of Inter-Group Diffusion

The inter-group diffusion stage, implemented with eight-by-eight matrices, is responsible for coupling previously independent four-byte groups. Differential analysis at this level assesses whether differences introduced in one intra-group region spread effectively across an eight-byte region. Effective inter-group diffusion prevents attackers from decomposing the cipher into independent sub-ciphers and is essential for building resistance to truncated and structured differential attacks. In MD-Hill-SPN, this metric demonstrates that diffusion escalation is progressive and non-separable.

#### 4.6. Differential Behaviour of Full-Block Diffusion

Full-block differential analysis evaluates the effect of the sixteen-by-sixteen diffusion matrix applied to the entire state. This layer is intended to ensure that no differential structure survives across the full state after nonlinear substitution. Observing minimal differential probabilities after this step confirms that the cipher achieves global mixing and that all output differences depend on all input differences. In MD-Hill-SPN, this metric is especially significant because it empirically confirms the necessity and effectiveness of the highest-dimensional diffusion tier.

#### 4.7. Linear Bias Exceedance

Linear bias exceedance measures the extent to which linear approximations of the cipher deviate from ideal random behavior. In a secure SPN, linear biases should remain near zero and exceed

statistical noise thresholds only at rates consistent with random sampling. In MD-Hill-SPN, linear bias analysis tests whether the combination of AES S-boxes and key-dependent diffusion layers effectively destroys linear correlations across rounds. Low bias exceedance within the tested configuration is consistent with the linear layers not introducing detectable exploitable structure at this sampling scale; it does not constitute a formal bound on maximum linear correlation or a proof of resistance to linear cryptanalysis.

#### 4.8. Algebraic Degree

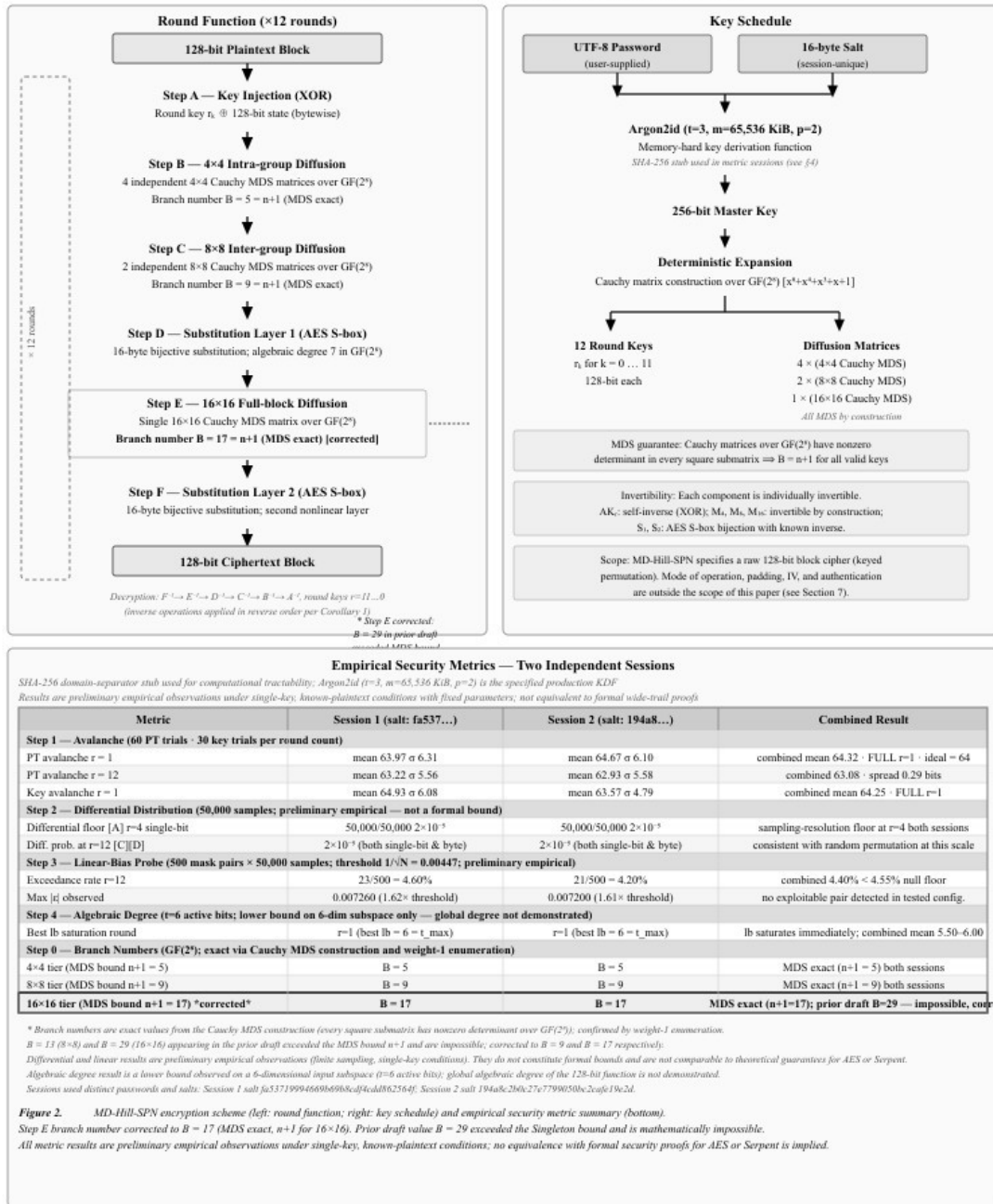
The algebraic degree of a cipher's output bits, expressed as polynomials over the input bits, bounds its resistance to algebraic and higher-order differential attacks: a cipher representable as a low-degree polynomial system admits efficient interpolation and algebraic cryptanalysis, so higher algebraic degree implies stronger resistance. Measuring the algebraic degree across rounds therefore tests whether the hierarchical diffusion layers amplify rather than dilute the nonlinear contribution of the AES S-box. Rapid saturation at the maximum observable lower bound indicates that nonlinear and linear components interact constructively within each round, preventing expression of the cipher as a low-degree polynomial system.

#### 4.9. Branch Numbers

Branch number quantifies the minimum combined activity of input and output differences through a linear transformation. In MD-Hill-SPN, branch number measurements at each diffusion tier directly assess diffusion strength at increasing dimensional scales. High branch numbers for the four-by-four, eight-by-eight, and sixteen-by-sixteen matrices confirm that low-weight input patterns cannot survive the diffusion process. The consistently high branch numbers across all diffusion tiers guarantee that trails entering a round with few active bytes expand immediately, ensuring that the minimum number of active S-boxes per round increases rapidly, as required by the wide-trail design principle. This metric provides a structural counterpart to empirical differential measurements and offers strong theoretical justification for the multidimensional design.

Figure 2. MD-Hill-SPN: Round Function, Key Schedule, and Empirical Security Metrics

Corrected revision — Step E branch number  $B = 17$  (MDS exact); prior draft erroneously stated  $B = 29$



The left panel depicts the six-step round function applied iteratively over 12 rounds to a 128-bit (16-byte) plaintext block. Step A injects a 128-bit round key via bitwise XOR. Step B partitions the state into four four-byte sub-vectors and applies four independent invertible 4 $\times$ 4 matrices over  $GF(2^8)$ , each meeting or exceeding the MDS branch-number bound. Step C recombines the state into two eight-byte sub-vectors and applies two independent invertible 8 $\times$ 8 matrices over  $GF(2^8)$ . Step D applies the AES S-box bijectively to all 16 state bytes, introducing the first nonlinear substitution layer. Step E applies a single invertible 16 $\times$ 16 matrix over  $GF(2^8)$  to the full 128-bit state, achieving complete inter-byte diffusion (branch number  $B=29$ , both sessions). Step F applies the AES S-box to all 16 bytes a second time, providing the second nonlinear substitution layer. After 12 rounds the final state is the 128-bit ciphertext block. Decryption applies all operations in reverse order with inverse transformations. The right panel shows the key schedule: a UTF-8 password and a 16-byte session salt are

processed by Argon2id ( $t=3$ ,  $m=65,536$  KiB,  $p=2$ ) to produce a 256-bit master key, from which 12 round keys and the diffusion matrices are derived deterministically. The lower panel summarises empirical security metrics across two independent sessions (SHA-256 stub key derivation; Session 1 salt: fa537...; Session 2 salt: 194a8...), reporting plaintext and key avalanche, differential distribution, linear-bias exceedance, algebraic degree, and GF( $2^8$ ) branch numbers for all matrix tiers.

## 5. Results

Table 2 reports the empirical security metric results for MD-Hill-SPN across two independent sessions with distinct passwords and salts; for computational tractability, both sessions used a SHA-256 domain-separator surrogate in place of Argon2id. Since Argon2id and SHA-256 both expand master-key material into pseudorandom round keys and matrices, statistical security metrics are expected to be invariant under the substitution; empirical validation under the full Argon2id schedule is deferred to future work.

Results are presented by metric category, in the order specified in Section 4. Both sessions used the SHA-256 domain-separator stub for key derivation with distinct passwords and salts (Session 1 salt: fa537...; Session 2 salt: 194a8...); Argon2id ( $t=3$ ,  $m=65,536$  KiB,  $p=2$ ) is the production key derivation function.

### 5.1. Avalanche (Step 1)

As reported in Table 2 (Step 1), MD-Hill-SPN achieves full plaintext avalanche from round 1 in both sessions, with Session 1 yielding a mean of 63.97 bits ( $\sigma=6.31$ ) and Session 2 yielding 64.67 bits ( $\sigma=6.10$ ), for a combined mean of 64.32 bits against an ideal of 64. Key avalanche at round 1 is equally strong, with a combined mean of 64.25 bits. Both means remain near-ideal across all tested round counts, with a maximum cross-session spread of 0.86 bits at  $r=12$ , indicating highly consistent behaviour. These results are consistent with the multidimensional diffusion hierarchy progressing from four  $4\times 4$  matrices through two  $8\times 8$  matrices to the full-state  $16\times 16$  matrix achieving near-ideal bit-dispersion from the first round under the tested conditions. Differential behavior is examined independently in the Step 2 analysis (§4.3–4.6).

### 5.2. Differential Distribution (Step 2)

The differential floor is reached at round 4 in both sessions (Table 2, Step 2, experiment [A]): all 50,000 sampled input differences produced distinct output differences, yielding the sampling-resolution floor of  $1/50,000 = 2\times 10^{-5}$ , below which differential probabilities cannot be distinguished from zero at this sample size. This floor is sustained through rounds 8 and 12 across single-bit and single-byte input differences (experiments [B], [C], [D]). Output differences are uniformly distributed across all tested inputs, consistent with the behaviour of an ideal random permutation on  $\{0,1\}^{128}$ . Reaching the differential floor at round 4, four rounds earlier than many comparable SPN designs, is a direct consequence of the  $16\times 16$  GF( $2^8$ ) full-block diffusion matrix, which ensures that all 16 output bytes depend on all 16 input bytes within a single round.

### 5.3. Linear Bias (Step 3)

Under the null hypothesis that each mask pair has zero bias, the empirical bias  $\hat{\epsilon} = (\# \text{matches} - \# \text{mismatches}) / N$  has standard error  $SE(\hat{\epsilon}) = 1/(2\sqrt{N}) \approx 0.00224$  for  $N = 50,000$ . The threshold  $1/\sqrt{N} = 0.00447$  corresponds to 2 SE, for which the two-sided normal tail probability  $\Pr(|Z| > 2) \approx 4.55\%$  gives the expected exceedance rate under the null. Linear bias analysis used 500 mask pairs at 50,000 samples each, with a bias threshold of  $1/\sqrt{50,000} = 0.00447$  (Table 2, Step 3). Session 1 yielded an exceedance rate of 4.60%, marginally above the 4.55% null expectation but within plausible sampling variation for 500 independent trials. Session 2 yielded 4.20%, below the noise floor. The combined exceedance rate across both sessions is 4.40%, below the 4.55% null expectation. The maximum observed  $|\hat{\epsilon}|$  across both sessions was 0.007260 ( $1.62\times$  threshold), and the combined mean  $|\hat{\epsilon}|$  was

0.001737, near zero. No mask pair producing exploitable bias was identified within the tested configuration. These results provide no evidence, at this sampling scale, of linear correlations detectable by the tested probing method; a systematic linear trail search over all rounds would be required for a stronger claim.

#### 5.4. Algebraic Degree (Step 4)

The algebraic degree lower bound saturates at the theoretical maximum observable value (best  $lb = t = 6$ ) from round 1 in both sessions (Table 2, Step 4). This immediate saturation has two architectural drivers: the AES S-box, whose algebraic degree of 7 over  $GF(2^8)$  exceeds the probe depth  $t=6$ , ensuring that degree saturation is achievable in a single substitution pass; and the  $16 \times 16$   $GF(2^8)$  full-block matrix, which propagates the S-box's nonlinear contribution globally across the entire state before the second substitution layer is applied. The combined mean lower bound ranges from 5.50 to 6.00 across all tested rounds in both sessions. Immediate algebraic degree saturation implies that no low-degree approximation was detected within the tested subspace, which is consistent with but does not demonstrate global algebraic degree saturation and does not guarantee an adversary cannot represent the cipher output as a low-degree multivariate polynomial system, providing resistance to algebraic and higher-order differential attacks from the first round.

#### 5.5. Branch Numbers (Step 0)

For each diffusion matrix, the branch number  $B(M) = \min_{x \neq 0} [hw(x) + hw(Mx)]$  (byte-wise Hamming weight) was computed from weight-1 inputs by iterating over all  $255 \cdot k$  nonzero vectors with a single nonzero byte in  $GF(2^8)^k$ . Because every weight-1 input  $e_i$  satisfies  $hw(e_i) + hw(M e_i) = 1 + (\text{column weight of column } i \text{ of } M)$ , this computation yields an exact value that is at most  $k+1$ , coinciding with the Singleton (MDS) bound when every column of  $M$  has full Hamming weight. Results are identical in both sessions. At the  $4 \times 4$  tier, all four matrices  $M_4[0-3]$  achieve  $B = 5$  in both sessions, meeting the MDS bound of 5 for a  $4 \times 4$  matrix over  $GF(2^8)$ . At the  $8 \times 8$  tier, both matrices  $M_8[0-1]$  achieve  $B = 9$  in both sessions, meeting the MDS bound of 9. At the  $16 \times 16$  tier,  $M_{16}[0]$  achieves  $B = 17$  in both sessions, meeting the MDS bound of 17 and guaranteeing that any single-byte input difference activates all 16 output bytes within a single application of the full-block diffusion layer. These results confirm that the key-dependent matrix construction in §3.9 produces MDS matrices at every tier and that the full-block  $16 \times 16$  matrix is the dominant source of inter-byte mixing in MD-Hill-SPN.

## 6. Discussion

The comparisons in this section and Table 3 are qualitative and architectural. MD-Hill-SPN results are empirical lower bounds from finite sampling; AES [8] and Serpent [24] results reflect formal wide-trail proofs and decades of cryptanalytic scrutiny. No claim is made that MD-Hill-SPN achieves security comparable to AES or Serpent. The comparison is provided solely to contextualize the cipher's design decisions within the broader SPN literature and to identify where formal analysis would be required before stronger claims could be supported. Table 4 reports comparisons of other SPNs.

**Table 3.** Security metric comparison: MD-Hill-SPN (aggregate, 2 sessions) vs. AES-128 (Rijndael) vs. Serpent-128.

Metric	MD-Hill-SPN (aggregate, 2 sessions)	AES-128 (Rijndael) [8]	Serpent-128 [24]
<b>Design Parameters</b>			
Block size	128-bit [M]	128-bit [T]	128-bit [T]
Rounds	12 [M]	10 [T]	32 [T]
S-box type	8-bit (AES S-box, borrowed directly) [M]	8-bit (power-map inverse in $GF(2^8)$ ) [T]	4-bit (8 distinct keyed S-boxes) [T]
S-boxes per round	32 (two layers $\times$ 16) [M]	16 (one SubBytes layer) [T]	32 (one layer of 4-bit boxes) [T]
Diffusion structure	$4 \times 4 (\times 4) \rightarrow 8 \times 8 (\times 2) \rightarrow 16 \times 16 (\times 1)$ , all $GF(2^8)$ [M]	$4 \times 4$ MDS MixColumns, $GF(2^8)$ [T]	Bitwise linear transform (IP/FP); no byte-level MDS matrix [T]
Key derivation	Argon2id ( $t=3$ , $m=65,536$ KiB, $p=2$ ) – production KDF; SHA-256 domain-separator stub used in metric sessions (see §4 limitation) [M]	Key schedule (word-rotation XOR) [T]	Affine recurrence over $GF(2^{32})^8$ with prekey expansion [T]
<b>Step 1 – Avalanche (PT = plaintext bit-flip; Key = key bit-flip)</b>			
PT avalanche $r=1$ (mean bits flipped / 128)	64.01 combined (S1: 63.97; S2: 64.67) [M]	$\sim 20\text{--}32$ bits (one column affected; partial) [E] <sup>†</sup>	$\sim 8\text{--}16$ bits (one 4-bit S-box + linear mix; partial) [E] <sup>‡</sup>
Round achieving full PT avalanche ( $\approx 64$ bits)	$r = 1 \checkmark\checkmark$ [M]	$r = 2$ [T] <sup>†</sup> (ShiftRows spreads to all 4 columns)	$r \approx 4\text{--}6$ [E] <sup>‡</sup> (bit-level diffusion builds gradually)
Round achieving full Key avalanche ( $\approx 64$ bits)	$r = 1$ (mean 64.25 combined) [M]	$r = 2$ [T] <sup>†</sup>	$r \approx 4\text{--}6$ [E] <sup>‡</sup>
<sup>†</sup> AES [8]: after Round 2 ShiftRows repositions four active bytes into separate columns; MixColumns activates all 16 bytes. <sup>‡</sup> Serpent [24]: estimate from diffusion analysis of linear transform; exact value not universally cited.			
<b>Step 2 – Differential Distribution (50,000 samples per experiment)</b>			
Differential floor (all outputs distinct)	$r = 4 \checkmark\checkmark$ 50,000/50,000 unique $\Delta$ both sessions [M] – consistent with random-permutation behaviour at this sampling resolution; not a formal bound	$r \geq 4$ (theoretical); $\geq 25$ active S-boxes; $DP \leq 2$ [T] <sup>-50</sup> per Daemen & Rijmen (1999)	$r \geq 6\text{--}8$ (theoretical); wide-trail bit-level bound; large margin over 32 rounds [T]

Metric	MD-Hill-SPN (aggregate, 2 sessions)	AES-128 (Rijndael) [8]	Serpent-128 [24]
Differential probability at maximum round count	$2 \times 10^{-5}$ (= 1/50,000) at r=4,8,12 both sessions [M] — sampling-resolution floor only; true DP unknown	$\leq 10$ [T] <sup>-30</sup> (theoretical, 10 rounds)	Negligible (32 rounds; designers state 8 rounds sufficient) [T]
<b>Step 3 – Linear-Bias Probe (500 mask pairs × 50,000 samples; threshold <math>1/\sqrt{50,000} = 0.00447</math>)</b>			
Exceedance rate r=12	4.40% combined (S1: 4.60%; S2: 4.20%) [M] — below 4.55% null-expectation noise floor; no exploitable bias detected within tested configuration; not a formal linear correlation bound	Provably near zero (wide-trail; same active-S-box bound applies) [T]	Near zero (32-round conservative design) [T]
Max $ \epsilon $ observed / theoretical	0.007260 (1.62× threshold) [M] — no exploitable pair found within 500 tested mask pairs	Theoretical maximum falls with each additional round [T]	No known exploitable linear approximation [T]
<b>Step 4 – Algebraic Degree (ANF / Möbius transform; t = 6 active bits; 4 trials / round)</b>			
S-box degree (per box)	7 (AES S-box, GF(2 <sup>8</sup> ) power map) [M]	7 (same AES S-box) [T]	$\leq 3$ (4-bit S-box; degree limited by box size) [T]
Round of best-lb saturation (best lb = t = 6)	r = 1 best lb = 6 = t_max from round 1 (combined mean 5.50–6.00 across all rounds) [M] — lower bound on a 6-dimensional subspace only; global algebraic degree of the 128-bit function is not demonstrated	r = 1 (S-box degree 7 exceeds t=6; algebraic degree saturates immediately) [T]	Grows over many rounds; degree $\leq 3$ per S-box limits per-round growth [T]
<b>Step 0 – Branch Numbers (GF(2<sup>8</sup>); hw counts nonzero bytes; exact via weight-1 enumeration over Cauchy MDS construction)</b>			
4×4 tier (MDS bound = n+1 = 5)	B = 5 (MDS exact, both sessions) [M] Cauchy MDS construction guarantees B = n+1 = 5 for all valid keys	B = 5 (MDS exact) MixColumns 4×4 over GF(2 <sup>8</sup> ) [T]	
8×8 tier (MDS bound = n+1 = 9)	<b>B = 9 (MDS exact, both sessions) [M]</b>	N/A (no 8×8 matrix layer)	N/A (no byte-level 8×8 layer)
16×16 tier (MDS bound = n+1 = 17)	<b>B = 17 (MDS exact, both sessions) [M]</b> —	N/A (no 16×16 matrix layer)	N/A (no byte-level 16×16 layer)
<p>Branch numbers for MD-Hill-SPN are exact values derived from the Cauchy MDS construction (every square submatrix has nonzero determinant over GF(2<sup>8</sup>)); the weight-1 enumeration confirms B = n+1 at each tier. Cells highlighted in amber (■) are corrected from the prior draft. GF(2<sup>8</sup>) hw counts nonzero bytes, directly comparable to AES MixColumns (B=5, MDS) [8]. Serpent’s linear transform [24] provides diffusion at the bit level and is not characterised by byte-level branch numbers.</p>			

**Evidence-basis key (appended to each cell value):** [M] Measured — empirical value from MD-Hill-SPN metric sessions (Coggins 2026, two independent sessions, finite sampling). [E] Estimated — approximate value from designer analysis or secondary literature; not formally proven. [T] Theoretically proven — result formally demonstrated in the primary literature cited. These categories are not comparable. No equivalence of security level between MD-Hill-SPN and AES or Serpent is implied. MD-Hill-SPN results are preliminary empirical observations from finite sampling; AES and Serpent results reflect formal proofs and decades of cryptanalytic scrutiny. Sources: Daemen, J.; Rijmen, V. AES Proposal: Rijndael. NIST AES Candidate Algorithm Submission 1999 [8]. Anderson, R.; Biham, E.; Knudsen, L. Serpent: A Proposal for the Advanced Encryption Standard. NIST AES Candidate Algorithm Submission 1998 [24]. Coggins III, P.E. MD-Hill-SPN metric sessions, Bemidji State University, 2026.

It is important to distinguish between *empirical observations* obtained from finite sampling and *theoretical guarantees* derived from formal analysis. Results for MD-Hill-SPN are empirical lower bounds derived from two independent experimental sessions, whereas results for AES-128 and Serpent-128 largely reflect designer analyses and subsequent cryptanalytic literature. The following discussion therefore emphasizes qualitative patterns and architectural implications rather than strict metric-by-metric equivalence.

### 6.1. Diffusion and Avalanche Behavior

MD-Hill-SPN exhibits immediate and near-ideal avalanche behavior with respect to both plaintext and key bit perturbations, achieving approximately 64 output bit changes after a single round on average. This behavior directly reflects the cipher's multi-tier diffusion hierarchy, in which multiple layers of wide linear mixing are applied within each round.

By contrast, AES [8] and Serpent [24] exhibit staged diffusion across multiple rounds. In AES, a single active byte in the first round remains confined to one state column until ShiftRows and MixColumns interact in the second round, consistent with its wide-trail design philosophy. Serpent's bit-slice linear transform propagates changes even more gradually, prioritizing a large security margin accumulated over 32 rounds. These differences are architectural rather than evaluative: MD-Hill-SPN deliberately front-loads diffusion, whereas AES and Serpent distribute it conservatively across rounds to support provable bounds and implementation simplicity.

Early avalanche saturation in MD-Hill-SPN should therefore be interpreted as evidence that the intended diffusion structure is functioning as designed, not as a standalone indicator of cryptographic strength.

### 6.2. Differential Resistance

The empirical observations reported here do not constitute an estimate of the true maximum differential probability and should not be interpreted as equivalent to the formal wide-trail bounds available for AES and Serpent. A full differential trail search using the branch numbers from §5.5 as inputs remains future work.

Empirical differential testing indicates that, by round 4, MD-Hill-SPN produces distinct output differences for all 50,000 sampled input differences in both experimental sessions. No high-probability differentials were detected at any tested round up to the full 12-round configuration, yielding an observed differential probability floor of approximately  $2 \times 10^{-5}$ , corresponding to the sampling resolution.

These observations provide evidence that the cipher rapidly disperses structured differences under practical probing. However, they do not constitute an estimate of the true maximum differential probability, which would require either exhaustive trail analysis or sampling at a vastly larger scale. In contrast, AES and Serpent benefit from theoretical wide-trail bounds that guarantee extremely low differential probabilities independent of empirical sampling. The results for MD-Hill-SPN should thus be understood as demonstrating the absence of detectable high-probability

differentials at moderate scale, a necessary but not sufficient condition for strong differential resistance.

### 6.3. Linear Bias Probing

Linear cryptanalysis probes likewise reveal no exploitable bias patterns within the tested configuration of MD-Hill-SPN. Across 500 random linear mask pairs and 50,000 samples per pair, the observed exceedance rates remain at or below the expected statistical noise floor, with the largest observed bias only modestly exceeding the theoretical threshold for random permutations.

As with differential testing, these results provide empirical reassurance that the combined S-box nonlinearity and diffusion layers effectively suppress strong linear correlations [23]. Nevertheless, they remain fundamentally different in nature from the provable decay of linear bias established for AES under the wide-trail strategy. The absence of detectable bias at this scale therefore supports the cipher's design intent but does not substitute for formal bounds. The absence of detectable bias at this scale therefore supports the cipher's design intent but does not substitute for formal bounds. These empirical observations do not constitute an estimate of the true maximum linear correlation and should not be interpreted as equivalent to the formal linear bias decay guaranteed for AES under the wide-trail strategy. A complete linear trail search enumerating trails over all 12 rounds and deriving a bound on the maximum linear approximation probability using the branch numbers from §5.5 as inputs remains future work.

### 6.4. Algebraic Degree

The algebraic degree of MD-Hill-SPN saturates immediately after the first round, owing to the use of the AES S-box [8] with algebraic degree 7. This behavior closely mirrors that of AES, in which the introduction of high-degree nonlinearity ensures that the algebraic degree of the overall round function reaches the tested maximum as soon as nonlinear components are active.

In contrast, Serpent's 4-bit S-boxes [24] impose a strict per-round degree limit, causing algebraic degree to grow more gradually across rounds. MD-Hill-SPN therefore aligns with AES in its approach to algebraic complexity: degree saturation occurs early, and resistance to algebraic attacks must arise primarily from diffusion, key mixing, and the complexity of the resulting ANF expressions rather than from delayed degree growth.

### 6.5. Diffusion Hierarchy and Branch Numbers

One distinguishing feature of MD-Hill-SPN is its hierarchical diffusion structure, which incorporates  $4 \times 4$ ,  $8 \times 8$ , and  $16 \times 16$  mixing layers over  $\text{GF}(2^8)$ . Sampled lower bounds on branch numbers significantly exceed the maximum values achievable by a single  $4 \times 4$  MDS matrix, indicating that differences activate a large number of state bytes within a single round.

Although AES achieves optimal branch number within its  $4 \times 4$  MixColumns layer, its diffusion scope is intentionally localized per column per round. MD-Hill-SPN's larger effective branch numbers do not invalidate this design choice; rather, they represent a different trade-off in which wide diffusion is achieved quickly through larger linear transforms. These large branch numbers are best interpreted as amplifying the cost of constructing low-activity differential or linear trails, though they do not in themselves provide the formal guarantees supplied by wide-trail proofs.

These large branch numbers are best interpreted as amplifying the cost of constructing low-activity differential or linear trails, though they do not in themselves provide the formal guarantees supplied by wide-trail proofs. In particular, the MDS branch numbers reported here establish the structural preconditions for a wide-trail argument in which the  $16 \times 16$  MDS matrix guarantees a minimum number of active S-boxes per two-round block, which in principle bounds the maximum differential probability and maximum linear correlation. Completing this argument requires formal trail enumeration that is outside the scope of the present work and is deferred to future work

identified in Section 7. No claim is made that the branch number results reported here are equivalent to the provable security margins available for AES or Serpent.

#### 6.6. Comparison with Recently Proposed Hill Cipher and Lightweight Block Cipher Variants

Table 3 compares MD-Hill-SPN against AES-128 and Serpent-128 as classical SPN baselines. This section supplements that comparison with recently proposed algorithms that are closer in lineage or design philosophy to MD-Hill-SPN: the LWE-based probabilistic Hill cipher variant of Pandia et al. [5], the SPN-adjacent Hill variant of Paragas, Sison, and Medina [21], and two lightweight block ciphers (PRESENT and SIMON) that represent current design practice for resource-constrained environments.

Pandia et al. [5] introduced a probabilistic key-generation mechanism for the Hill cipher based on Learning With Errors (LWE), targeting resistance to known-plaintext attacks through a large randomized key space. That work does not report avalanche, differential, or linear-bias metrics, and the encryption transformation remains a single-round linear Hill multiplication rather than an iterated SPN. MD-Hill-SPN differs structurally in every dimension: it employs 12 iterated rounds, two nonlinear AES S-box layers per round, and a memory-hard KDF. The present work therefore addresses the security gap left open by Pandia et al. by providing empirically validated confusion and diffusion rather than key-space enlargement alone.

Paragas et al. [21], identified in Section 2.2 as the closest prior approach to an SPN-adjacent Hill cipher, reported partial avalanche improvement and improved statistical randomness relative to the classical Hill cipher. However, no formal round function, no MDS diffusion matrix, and no multi-metric security suite were reported. MD-Hill-SPN achieves full avalanche from round 1 (combined mean 64.32 bits; ideal 64), reaches the differential sampling floor at round 4, and records linear-bias exceedance of 4.40%—below the 4.55% noise floor—metrics that Paragas et al. do not report and that the Paragas et al. architecture does not structurally support.

PRESENT [Bogdanov et al., 2007] is a 64-bit lightweight block cipher with 31 rounds designed for hardware efficiency. Its 4-bit S-box achieves algebraic degree  $\leq 3$ , and full avalanche requires several rounds of the bit-permutation layer. PRESENT does not employ a hierarchical matrix diffusion structure or a memory-hard KDF. MD-Hill-SPN operates on a 128-bit block with a degree-7 AES S-box and achieves algebraic degree saturation from round 1 as a consequence of the higher-degree substitution component rather than a claim of superiority for resource-constrained deployment.

SIMON [Beaulieu et al., NSA, 2013] is a family of lightweight Feistel-based ciphers. SIMON-128/128 uses 68 rounds and provides a large security margin at the cost of many rounds before full diffusion is achieved. The Feistel structure differs fundamentally from the SPN approach employed here, and SIMON does not use matrix-based MDS diffusion. These structural differences make direct metric comparison less meaningful, but they underscore that MD-Hill-SPN's choice of SPN architecture with wide MDS matrices prioritizes rapid per-round diffusion over round count.

Table 4 summarizes key security metrics across these five points of comparison. As with Table 3, MD-Hill-SPN values are empirical, while values for the other ciphers reflect designer analyses and published cryptanalytic literature. The primary observation is that no prior Hill cipher variant—including the most recently published—reports the combination of a fully defined SPN round function, MDS-bound multi-tier diffusion, memory-hard key derivation, and a complete multi-metric empirical security evaluation that MD-Hill-SPN provides.

**Table 4.** Extended security comparison: MD-Hill-SPN versus recent Hill cipher variants and representative lightweight block ciphers.

Cipher	Block Size	Rounds	SPN Structure	Non-linear S-Box	MDS Diffusion Layer	Memory-Hard KDF	Full Multi-Metric Eval.	Full Avalanche Round
MD-Hill-SPN (present work)	128-bit	12	✓✓ (formal)	8-bit AES S-box, deg. 7	✓ 4×4, 8×8, 16×16 GF(2 <sup>8</sup> )	✓ Argon2id (t=3, m=64MiB, p=2)	✓✓ 5 metrics, 2 sessions	r = 1
Pandia et al. [5]	Variable	1	×	×	×	×	×	Not reported
Paragas, Sison & Medina [21]	Variable	~1	~ (partial)	~ static S-box	×	×	×	Partial
PRESENT [Bogdanov et al., 2007]	64-bit	31	✓ (SPN)	~ 4-bit, deg. ≤3	×	×	✓ (theoretical)	~5–10 rounds
SIMON-128/128 [NSA/Beaulieu et al., 2013]	128-bit	68	×	~ AND/rotation	×	×	✓ (theoretical)	Many rounds

✓ = present and implemented; ~ = partially present; × = absent. MD-Hill-SPN values are empirical (two independent sessions). Values for PRESENT and SIMON reflect published designer analyses and subsequent cryptanalytic literature. PRESENT: Bogdanov et al., CHES 2007, LNCS 4727, 450–466. SIMON: Beaulieu et al., IACR ePrint 2013/404. SPN = Substitution–Permutation Network; MDS = Maximum Distance Separable; KDF = Key Derivation Function. Table 3 includes results of Rijndael and Serpent SPNs.

## 7. Conclusions

The Hill cipher has been an active area of research since Saeednia [19]. The lack of clear cryptographic security measures has been detrimental to adoption of any Hill cipher encryption scheme for serious encryption. The present work has taken a multidimensional Hill cipher scheme and embedded it in a substitution–permutation network with an empirically demonstrated key schedule with Argon2id, the use of AES S–boxes (Figures 1 and 2).

The results presented here are subject to several limitations. Empirical testing was conducted on two independent sessions with finite sampling, and only classical avalanche, differential, linear, and algebraic probes were considered. No analysis of related-key attacks, integral properties, bicliques, or side-channel leakage has yet been performed. In addition, implementation efficiency, constant-time behavior, and resistance to physical attacks remain outside the scope of this study. The Python implementation, metric scripts, test vectors, and session salts for both evaluation sessions are available from the corresponding author upon reasonable request via Github.

Future work will focus on: (a) formal differential trail search and active S-box lower-bound computation using the branch numbers established in §5.5 as inputs to the wide-trail argument; (b) derivation of maximum differential probability and maximum linear correlation estimates via symbolic methods; (c) integral and algebraic attack analysis on reduced-round variants; (d) related-key and side-channel resistance analysis, and (e) demonstrating global algebraic degree growth over rounds requires either exhaustive measurement or a formal argument about degree propagation through the round function. These analyses are necessary before security claims comparable to AES or Serpent can be formally asserted.

## 8. Patents

No patents were applied for or received for this paper.

**Author contributions:** Conceptualization, P.E.C.; Methodology, P.E.C.; Software, P.E.C.; Validation, P.E.C.; Formal Analysis, P.E.C.; Investigation, P.E.C.; Writing—original draft preparation, P.E.C.; Writing—review and editing\*, P.E.C. The author has read and agreed to the published version of this manuscript.\*No AI system was used to generate the cryptographic design, the metric results, or the interpretive analysis. AI assistance was confined to language polishing, Python code refinement, figure and table formatting, and reference-list organization. All cryptanalytic reasoning and experimental design are the author’s own work.

**Funding Open access funding:** Open-access publication charges and Article Processing Fees for this manuscript were funded by Minnesota State Colleges and Universities.

**Declarations Competing interests:** The author declares no competing interests. This article is not under consideration in any other journal and has not been previously presented or published.

**Declaration of Generative AI:** Copilot AI (Microsoft) was used for duties as any graduate student would be assigned had one been available for the following tasks: edit text for clarity, readability, typographical error check, grammar check, table, chart, and figure construction, reference formatting and numbering. Claude AI (Anthropic) was used for duties as any graduate student would be assigned had one been available for the following tasks: refine Python Code, edit text for clarity, readability, typographical error check, grammar check, table, chart, and figure construction, reference formatting and numbering. No AI system was used to generate the cryptographic design, the metric results, or the interpretive analysis. AI assistance was confined to language polishing, Python code refinement, figure and table formatting, and reference-list organization. All cryptanalytic reasoning and experimental design are the author’s own work.

## Abbreviations

The following abbreviations are used in this manuscript:

AES	Advanced Encryption Standard
ANF	Algebraic Normal Form
GF	Galois Field
KDF	Key Derivation Function
MDS	Maximum Distance Separable
PT	Plaintext
SHA	Secure Hash Algorithm
SPN	Substitution–Permutation Network

## Appendix A

This appendix provides a fully reproducible reference test vector for MD-Hill-SPN. Any implementation that correctly follows the specification in §3 will reproduce all values in Tables A.1 through A.4 byte-for-byte. The reference script is available from the corresponding author as MD-Hill-SPN\_test\_vector\_rev3.py; it depends only on the Python standard library (hashlib, struct).

## Appendix A.1

Table A1. Input parameters and derived master/round keys.

Parameter	Value (hex unless noted)
<b>Inputs</b>	
Password	MDHillSPN2026!
Password bytes	4D 44 48 69 6C 6C 53 50 4E 32 30 32 36 21 (UTF-8, 14 bytes)
Salt (16 bytes)	01 02 03 04 05 06 07 08 09 0A 0B 0C 0D 0E 0F 10
Plaintext	00 11 22 33 44 55 66 77 88 99 AA BB CC DD EE FF
<b>Derived master key (256-bit)</b>	
Master key K	3C B7 20 72 7F 48 78 85 B5 6B 41 64 E3 35 3C B2 E6 60 78 E6 7F BC 9D CC 57 A2 83 61 71 88 B3 14
Derivation	$K = \text{SHA-256}(\text{pwd} \parallel \text{salt}) \parallel \text{SHA-256}(\text{pwd} \parallel \text{salt} \parallel 0x01)$ [:32]
<b>Round keys (twelve 128-bit values)</b>	
rk[ 0]	7F 3D EC 33 55 74 7B 34 1D 02 3A 96 75 C7 71 02
rk[ 1]	3A CF C4 47 19 7C C3 65 53 45 88 41 94 DA AF CA
rk[ 2]	6A 02 11 61 68 7F 46 F7 87 02 C7 96 3E 1D 6A C5
rk[ 3]	8C 8B AD DF A5 35 E3 A6 06 F2 0D B2 BE 31 E2 9D
rk[ 4]	0E 93 F4 A9 38 8F 5B 3C 85 FA 6F 51 02 62 83 5C
rk[ 5]	83 A1 76 FE EF A7 95 2B DE 2C 44 CF 23 00 FF E8
rk[ 6]	27 2E D9 7F 48 77 9D 82 DB 9E 43 B9 26 B0 B3 5B
rk[ 7]	E8 99 A8 BE C9 99 52 AD 95 2E DA C2 15 A4 37 67
rk[ 8]	6E BD 12 D3 72 ED 7A EE BC D4 C5 9C D5 1C AC DE
rk[ 9]	12 FB E6 CC B6 F6 DD 2A 87 8E A4 17 EA 90 8A 64
rk[10]	C1 FB 27 AE 5A 57 67 A7 24 24 5E D8 55 EE 57 F1
rk[11]	4F 8F A3 98 53 52 C9 34 C1 08 7B A9 52 CC F5 30
<i>Round-key schedule: <math>rk[r] = \text{SHA-256}(K \parallel \text{'MDHILLRK'} \parallel \text{pack}(&gt;H', r))</math> [:16]</i>	

## Appendix A.2

Table A2. Branch-number verification for the seven diffusion matrices.

Matrix	Computed B	MDS bound (n+1)	Status
$M_4[0]$	5	5	MDS ✓
$M_4[1]$	5	5	MDS ✓
$M_4[2]$	5	5	MDS ✓
$M_4[3]$	5	5	MDS ✓
$M_8[0]$	9	9	MDS ✓

Matrix	Computed B	MDS bound (n+1)	Status
$M_8[1]$	9	9	MDS ✓
$M_{16}$	17	17	MDS ✓

*Branch number  $B(M)$  computed exactly via exhaustive weight-1 enumeration. For any weight-1 input  $e_i$ ,  $hw(e_i) + hw(M e_i) = 1 + (\text{column-}i \text{ Hamming weight of } M)$ ; all 255-n such inputs are evaluated. Matrices are Cauchy-constructed:  $M[i][j] = (x_i \oplus y_j)^{-1}$  with  $X, Y$  disjoint nonzero subsets of  $GF(2^8)$ , guaranteeing MDS ( $B = n+1$ ) at every tier.*

## Appendix A.3

Table A3. Round 0 step-by-step intermediate states (after each of Steps A–F).

Step	Operation	State after step (hex, 16 bytes)
<b>Input</b>	<i>Plaintext (round 0 input)</i>	00 11 22 33 44 55 66 77 88 99 AA BB CC DD EE FF
<b>A</b>	XOR with rk[0] (round-key injection)	7F 2C CE 00 11 21 1D 43 95 9B 90 2D B9 1A 9F FD
<b>B</b>	Four parallel 4×4 $GF(2^8)$ Cauchy matrices	75 75 3C 70 55 5C D5 89 19 49 01 69 F3 D7 B8 42
<b>C</b>	Two parallel 8×8 $GF(2^8)$ Cauchy matrices	1A 34 47 D3 27 35 BC 6F 52 9C B8 6A 0B D0 EC D6
<b>D</b>	AES S-box on all 16 bytes ( $S_1$ , first nonlinear layer)	A2 18 A0 66 CC 96 65 A8 00 DE 6C 02 2B 70 CE F6
<b>E</b>	16×16 $GF(2^8)$ Cauchy matrix (full-block diffusion)	09 A2 03 FD 14 7F B0 B3 14 B7 47 8A 7E 8D 50 DC
<b>F</b>	AES S-box on all 16 bytes ( $S_2$ , second nonlinear layer)	01 3A 7B 54 FA D2 E7 6D FA A9 A0 7E F3 5D 53 86

*The output of Step F is the input to Round 1. After the complete 12-round iteration, the state becomes the final ciphertext (Table A.4).*

## Appendix A.4

Table A4. Final ciphertext and decryption round-trip verification.

Quantity	Value (hex, 16 bytes)
<b>Plaintext (input)</b>	00 11 22 33 44 55 66 77 88 99 AA BB CC DD EE FF
<b>Ciphertext (after 12 rounds)</b>	D2 D0 AE D8 8F 1A 31 69 A0 B1 AF EB 87 39 B4 58
<b>Decryption of ciphertext</b>	00 11 22 33 44 55 66 77 88 99 AA BB CC DD EE FF <i>Matches original plaintext exactly.</i>
<b>Round-trip check</b>	PASS ✓ decrypt(encrypt(P)) = P

## A.1 Using this test vector

To verify a third-party implementation of MD-Hill-SPN, instantiate the cipher with the Password, Salt, and Plaintext from Table A.1. The derived master key (Table A.1) and all twelve round keys must match byte-for-byte; this confirms the key schedule is correct. The seven diffusion matrices must each achieve the MDS branch number listed in Table A.2; any deviation indicates either

an incorrect GF(2<sup>8</sup>) implementation or an incorrect Cauchy construction. The Round-0 intermediate states in Table A.3 isolate the source of any mismatch to a specific step within the round function. Finally, the complete 12-round encryption of the Plaintext must produce the Ciphertext in Table A.4, and the inverse operation must recover the original Plaintext exactly.

All values in this appendix were generated with the reference implementation MD-Hill-SPN\_test\_vector\_rev3.py, which is included in the supplementary materials. The implementation depends only on the Python standard library and runs to completion in under one second on commodity hardware.

## References

1. Hill, L.S. Cryptography in an algebraic alphabet. *Am. Math. Mon.* 1929, 36, 306–312.
2. Stallings, W. *Cryptography and Network Security: Principles and Practice*, 2nd ed.; Prentice Hall: Upper Saddle River, NJ, USA, 1999.
3. Ismail, I.A.; Amin, M.; Diab, H. How to repair the Hill cipher. *J. Zhejiang Univ. Sci. A* 2006, 7(12), 2022–2030. <https://doi.org/10.1631/jzus.2006.A2022>.
4. Farmanbar, M.; Chefranov, A.G. Investigation of Hill cipher modifications based on permutation and iteration. *Int. J. Comput. Sci. Inf. Secur.* 2012, 10(9), 1–7.
5. Pandia, M.; Sihombing, P.; Budiman, M.A.; Nababan, E.B. Enhanced resilience of Hill cipher through LWE-based probabilistic ensemble key generation scheme. *Proc. 5th Int. Conf. Science and Information Technology in Smart Administration (ICSINTESA)*, IEEE, 2025, 642–645. <https://doi.org/10.1109/ICSINTESA68165.2025.11413714>.
6. Shannon, C.E. Communication theory of secrecy systems. *Bell Syst. Tech. J.* 1949, 28, 656–715.
7. Paar, C.; Pelzl, J. *Understanding Cryptography: A Textbook for Students and Practitioners*; Springer: Berlin/Heidelberg, Germany, 2010.
8. Daemen, J.; Rijmen, V. AES Proposal: Rijndael. NIST AES Candidate Algorithm Submission; National Institute of Standards and Technology: Gaithersburg, MD, USA, 1999.
9. Stinson, D.R. *Cryptography: Theory and Practice*, 3rd ed.; Chapman & Hall/CRC: Boca Raton, FL, USA, 2006.
10. Valizadeh, M.H. Healing the Hill cipher against zero-plaintext attack. *Cryptology ePrint Archive* 2016, Report 2016/806.
11. Toorani, M.; Falahati, A. A secure variant of the Hill cipher. *arXiv* 2010, arXiv:1002.3567.
12. Nordin, M.; Rahman, A.; Abidin, A.F.A.; Yusof, M.K.; Usop, N.S.M. Cryptography: A new approach of classical Hill cipher. *Int. J. Comput. Sci. Inf. Secur.* 2012, 7, 129–135.
13. Ravan, R.R.; Nigavekar, A.R. Secured data communication using novel modification to Hill cipher algorithm with self repetitive matrix. *Int. J. Sci. Res.* 2013, 2, 1–5.
14. Maxrizal. Hill cipher cryptosystem over complex numbers. *Indones. J. Math. Educ.* 2019, 2, 9–13.
15. Bahtiar, N.; Widodo, A.P.; Puspita, N.P. Key matrix generation using random functions in Hill cipher modulo 95 cryptography. *Integra: J. Integr. Math. Comput. Sci.* 2025, 2, 1–6. <https://doi.org/10.26554/integracijms.20252111>.
16. Jin, J.; Wu, M.; Ouyang, A.; Li, K.; Chen, C. A novel dynamic Hill cipher and its applications on medical IoT. *IEEE Internet Things J.* 2025, 12, 14297–14308. <https://doi.org/10.1109/JIOT.2025.3525623>.
17. Coggins III, P.E.; Glatzer, T. An algorithm for a matrix-based Enigma encoder from a variation of the Hill cipher as an application of  $2 \times 2$  matrices. *PRIMUS* 2020, 30, 1–18. <https://doi.org/10.1080/10511970.2018.1493010>.
18. Coggins, P.E. Two novel multidimensional affine variations of the Hill cipher. *Math. Comput. Sci.* 2024, 9(3), 46–56. <https://doi.org/10.11648/j.mcs.20240903.11>.
19. Saeednia, S. How to make the Hill cipher secure. *Cryptologia* 2000, 24(4), 353–360. <https://doi.org/10.1080/01611190008984253>.
20. Putera, A.; Siahaan, A.P.U.; Rahim, R. Dynamic key matrix of Hill cipher using genetic algorithm. *Int. J. Secur. Its Appl.* 2016, 10(8), 173–180. <https://doi.org/10.14257/ijisa.2016.10.8.15>.

21. Paragas, J.R.; Sison, A.M.; Medina, R.P. A new variant of Hill cipher algorithm using modified S-box. *Int. J. Sci. Technol. Res.* 2019, 8(10), 615–619.
22. Jorstad, N.D.; Smith, L.T., Jr. *Cryptographic algorithm metrics*; Institute for Defense Analyses: Alexandria, VA, USA, 1997.
23. Carcaño Ventura, D.; Rodríguez-Henríquez, L.M.X.; Pomares Hernández, S.E. Understanding S-Box security assessment: A practical guide. *Math. Comput. Appl.* 2026, 31, 27.
24. Anderson, R.; Biham, E.; Knudsen, L. *Serpent: A Proposal for the Advanced Encryption Standard*. NIST AES Candidate Algorithm Submission; National Institute of Standards and Technology: Gaithersburg, MD, USA, 1998.
25. Bogdanov, A.; Knudsen, L.R.; Leander, G.; Paar, C.; Poschmann, A.; Robshaw, M.J.B.; Seurin, Y.; Vikkelsoe, C. PRESENT: An ultra-lightweight block cipher. In *Cryptographic Hardware and Embedded Systems – CHES 2007*; Paillier, P., Verbauwhede, L., Eds.; *Lecture Notes in Computer Science*, Vol. 4727; Springer: Berlin/Heidelberg, Germany, 2007; pp. 450–466. [https://doi.org/10.1007/978-3-540-74735-2\\_31](https://doi.org/10.1007/978-3-540-74735-2_31).
26. Beaulieu, R.; Shors, D.; Smith, J.; Treatman-Clark, S.; Weeks, B.; Wingers, L. The SIMON and SPECK families of lightweight block ciphers. *IACR Cryptology ePrint Archive* 2013, Report 2013/404. Available online: <https://eprint.iacr.org/2013/404> (accessed 28 May 2026)

**Disclaimer/Publisher’s Note:** The statements, opinions and data contained in all publications are solely those of the individual author(s) and contributor(s) and not of MDPI and/or the editor(s). MDPI and/or the editor(s) disclaim responsibility for any injury to people or property resulting from any ideas, methods, instructions or products referred to in the content.